3B2-1

Analysis of Eccentric Dipole Antenna in Cylindrical Layers for Borehole Radar Applications

#Satoshi Ebihara, Yoshihiro Inoue
Faculty of Engineering, Osaka Electro-Communication University
18-8 Hatsu-cho, 572-8530, Neyagawa, JAPAN, s-ebihara@m.ieice.org

1. Introduction

Borehole radar is a form of ground-penetrating radar, which is a popular method for high-resolution imaging of the shallow subsurface. Boreholes are usually filled with fluid such as water, and this medium fills the space between the antennas and the formation. Many authors have reported that the structure influences the measured data in borehole radar. In the works [1]-[3], they assumed that the sonde including the antennas is located on the center of the borehole. However, the sonde is not always centered in a borehole in actual measurement.

In an induction logging tool, eccentered tool have been already investigated. Lovell and Chew have derived an efficient algorithm to solve the problem of an eccentered induction tool, with or without a metallic mandrel, in the presence of an inhomogeneous multicylindrically layered formation [4]. Hue and Teixeira extend it to tilted coil antennas in eccentric formation [5]. We may extend these works for the borehole radar case.

In this paper, we will derive the field of a point electric dipole, which is eccentered in a borehole. With this function included in MoM, we model the eccentric dipole antenna in a borehole. In order to verify the driven algorithm, an experiment was done. Throughout the paper, the time factor $\exp(-i\omega t)$ is assumed and suppressed.

2. Calculation of Fields of Electric Point Source for MoM Analysis

A theoretical model for a thin dipole antenna in homogeneous media can be derived from the Method of Moment (MoM) using Green's function G_0. In the presence of special scattering medium, we can evaluate the impedance matrix including the scattered field by substituting the free space Green's function G_0 with G_d , which includes the scattered filed, in the MoM [1]-[3].

In this paper, we will extend analytical methods in [4]-[5] and derive field of a pint electrical dipole source. This is equivalent to derivation of the Green's function G_d. Now, we consider a point electric dipole covered with a cylindrical insulator. The crosssection of the medium is like in Fig. 1. The diameters of the cylindrical layers are $2a_1$ and $2a_2$, respectively. The origin O is located on the center of the outermost cylindrical layer, and another origin O'' is on the center of the innermost cylindrical layer. The point electric dipole is pointing z direction on the z''-axis. The z components of the electric field and the magnetic filed in region 2 can be decomposed into spectral

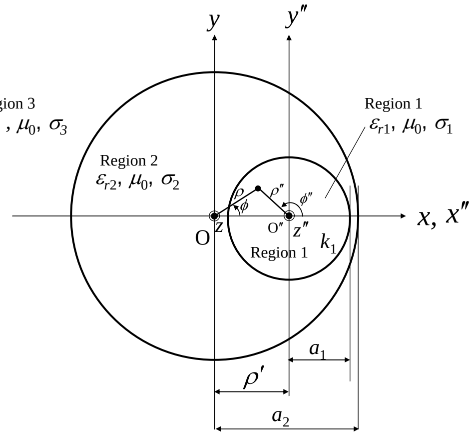

Figure 1: Crosssection of the cylindrical layers.

ISBN: 978-4-88552-223-9 C3055©IEICE

components $\left[E_{2z} \quad H_{2z}\right]^T$ having the *z*-component k_z of the wave number vector as

$$\begin{bmatrix} E_{2z} \\ H_{2z} \end{bmatrix} = \sum_{n''} e^{in\phi''} \left[\left\{ H_{n''}^{(1)}(k_{2\rho}\rho'')\mathbf{R}_{21}^{(n'')} + J_{n''}(k_{2\rho}\rho'')\mathbf{I} \right\} \mathbf{a}_2^{(n'')} + H_0^{(1)}(k_{2\rho}\rho'')\mathbf{T}_{12}^{(n''=0)} \begin{bmatrix} k_{1\rho}^2 \\ 0 \end{bmatrix}, \tag{1}$$

where the matrix $\mathbf{T}_{ij}^{(n)}$ and $\mathbf{R}_{ij}^{(n)}$ are the *n*-th order 2×2 transmission matrix and 2×2 reflection matrix at cylindrical boundaries between region *i* and *j*, respectively, and these are given in [6, Chapter 3]. The matrix $\mathbf{I}$ is an identity matrix. The radial component of the wave number is given by $k_{i\rho} = \sqrt{k_i^2 - k_z^2}$ $(i = 1,2,3)$ and k_i is the wave number of a plane wave in the *i*-th layer. $\mathbf{a}_2^{(n)}$ is an unknown arbitrary column vector. With the addition theorem [6, Appendix D], the above equation is decomposed around the *z*-axis, and we rewrite (1) as

$$\begin{aligned} \begin{bmatrix} E_{2z} \\ H_{2z} \end{bmatrix} = \sum_{n} e^{in\phi} \Bigg[\Bigg\{ \Bigg(\sum_{n''} J_{n-n''}(k_{2\rho}\rho')\mathbf{R}_{21}^{(n'')}\mathbf{a}_2^{(n'')} \Bigg) + J_n(k_{2\rho}\rho')\mathbf{T}_{12}^{(n''=0)} \begin{bmatrix} k_{1\rho}^2 \\ 0 \end{bmatrix} \Bigg\} H_n^{(1)}(k_{2\rho}\rho) \\ + \Bigg(\sum_{n''} J_{n-n''}(k_{2\rho}\rho')\mathbf{I}\mathbf{a}_2^{(n'')} \Bigg) J_n(k_{2\rho}\rho) \Bigg] \qquad (\rho' < \rho) \end{aligned} . \tag{2}$$

In the region 2, there are both standing wave and outgoing waves, and the fields should be the form of

$$\begin{bmatrix} E_{2z} \\ H_{2z} \end{bmatrix} = \sum_{n} e^{in\phi} \left[H_n^{(1)}(k_{2\rho}\rho)\mathbf{I} + J_n(k_{2\rho}\rho)\mathbf{R}_{23}^{(n)} \right] \mathbf{b}_2^{(n)} . \tag{3}$$

The vector $\mathbf{b}_2^{(n)}$ is an unknown arbitrary column vector. By comparing (2) and (3), we have two equations. Eliminating $\mathbf{b}_2^{(n)}$, we have

$$J_n(k_{2\rho}\rho')\mathbf{R}_{23}^{(n)}\mathbf{T}_{12}^{(n''=0)} \begin{bmatrix} k_{1\rho}^2 \\ 0 \end{bmatrix} = \sum_{n''} J_{n-n''}(k_{2\rho}\rho') \left\{ \mathbf{I} - \mathbf{R}_{23}^{(n)}\mathbf{R}_{21}^{(n'')} \right\} \mathbf{a}_2^{(n'')} . \tag{4}$$

These system equations can be solved for the vector $\mathbf{a}_2^{(n)}$, from which the *z*-component of the field in region 1 can be given by

$$\begin{bmatrix} E_{1z} \\ H_{1z} \end{bmatrix} = \left[H_0^{(1)}(k_{1\rho}\rho'')\mathbf{I} + J_0(k_{1\rho}\rho'')\mathbf{R}_{12}^{(n''=0)} \right] \begin{bmatrix} k_{1\rho}^2 \\ 0 \end{bmatrix} + \sum_{n''} e^{in''\phi''} J_{n''}(k_{1\rho}\rho'')\mathbf{T}_{21}^{(n'')}\mathbf{a}_2^{(n'')} . \tag{5}$$

When the source is a point electric dipole at $(\rho'' = 0, z')$ pointing *z* direction, integrating the $\left[E_{1z} \quad H_{1z}\right]^T$ with respect to k_z, the *z*-components E_z and H_z of the total fields at $(\rho'', z), (a_1 > \rho'')$ are given as

$$\begin{aligned} \begin{bmatrix} E_z \\ H_z \end{bmatrix} = \frac{i}{4\pi\omega\varepsilon_1} \sum_{n''} e^{in''\phi''} \int_{-\infty}^{\infty} e^{ik_z(z-z')} dk_z \\ \frac{i}{2} \left\{ \delta_{n'',0} \left[H_0^{(1)}(k_{1\rho}\rho'')\mathbf{I} + J_0(k_{1\rho}\rho'')\mathbf{R}_{12}^{(n''=0)} \right] \begin{bmatrix} k_{1\rho}^2 \\ 0 \end{bmatrix} + J_{n''}(k_{1\rho}\rho'')\mathbf{T}_{21}^{(n'')}\mathbf{a}_2^{(n'')} \right\} \end{aligned} . \tag{6}$$

where $\delta_{n'',0} = 1(n'' = 0), 0(n'' \neq 0)$. ε_1 is the permittivity in region1. In (6), we assumed that the product of the current *I* and the length *l* of the source is one, *i.e.* $Il = 1$. We should notice that the values of the total field E_z corresponds to that of the Green's functions $G_d(\phi, z, \phi', z')$ in (10) in [1], except for the values of ρ and ρ' . This implies that we may model single eccentered dipole antenna in a borehole with (6) and the MoM. Although the dipole antenna array is considered in [1], note that we consider single dipole antenna case, which is much more common, in this paper.

3. Numerical Results and Experimental Verification

Now we consider an eccentric dipole antenna in three cylindrical layers as shown in Fig. 2. Note that Fig. 1 is equivalent to the crosssection of Fig. 2, except for existence of the dipole antenna. The dipole antenna is located on the z'' axis. The red lines in Fig. 3 show the calculated input impedances with the MoM. Above 400 MHz, we can see some differences among the three cases, *i.e.* an antenna in homogeneous medium, one centered in cylindrical layers and one eccentered. We modeled the dipole antenna, which is insulated by medium such as FRP, in the MoM. We may regard the air in the innermost cylindrical layer in the model as the insulator in the actual borehole radar. Note that the dipole antenna is always centered in the innermost cylindrical layer both in the model and the actual borehole radar measurement. The borehole is usually filled with water in actual borehole radar, and we model the water layer in the second layer in the MoM. If there is the water layer around the antenna, the input impedance changes with the frequencies sharply. It should be noted that the resonant frequencies caused by the total length *l* are different among the three cases. We should notice the highest operating frequency in actual borehole radar measurement is about 500 MHz, and the most common ones are usually between 10 MHz and 200 MHz. The outermost layer is rock or soil in the actual borehole radar measurement, instead of the air in the model of the MoM. The relative permittivity of the rock or soil is usually between 7 and 30. Since permittivity of the rock or the soil is higher than that of air, the resonance frequency would be lower in actual borehole radar measurement than in the MoM model. According to the MoM calculation, the antenna impedance would be changed by the condition which includes eccentricity of the antenna in the common frequencies of the borehole radar.

For experimental verification, we did experiments with a monopole antenna on a ground plane as shown in Fig. 4. We imitated the model of the MoM in the experiments. The water layer was made by thin acryl pipes and pure water. We prepared the two types of the acryl pipes with the different distance ρ' for the centered dipole antenna and the eccentered dipole antenna. The blue lines in Fig. 3 show the measured data. We find that each experimental curve is similar to corresponding one in MoM. We verified the proposed equation (6).

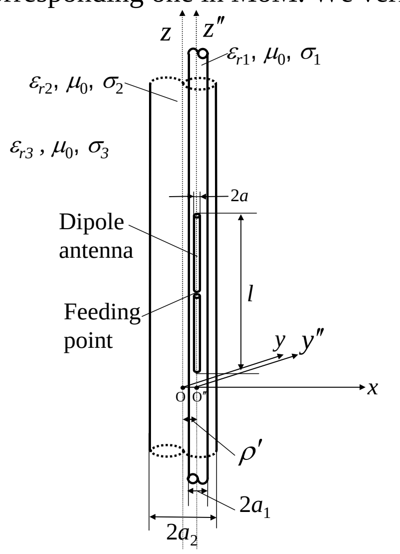

Figure 2: Coordinate system used to describe the geometry of the problem.

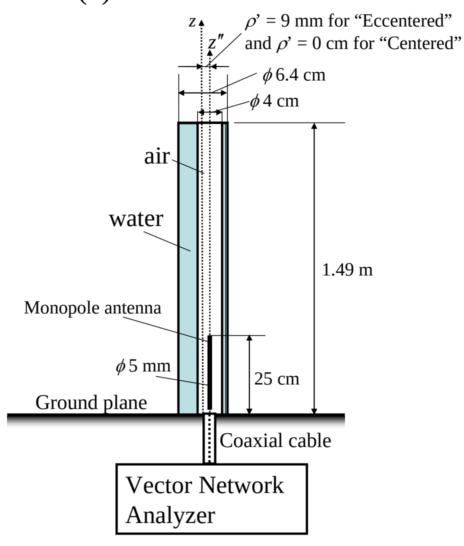

Figure 4: Measurement of input impedance of the monopole antenna.

4. Conclusions

We derived analytical fields of the electric point source in order to model a dipole antenna, which is eccentered in cylindrical layer, with the MoM. This condition can be seen in actual borehole radar measurement, since the sonde including the antenna is usually eccentered in deep depth. In the derivation, we extended the previous works [4]-[5] to the electric dipole case, and we may model the eccentric dipole antenna. According to the calculation with the MoM, we found that the eccentricity of the antenna significantly affect the antenna impedance. We verified the calculation with the measured input impedance of the monopole antenna on the ground plane.

Acknowledgments

We would like to thank T. Kajiwara and C. Oono for development of the ground plane. This work was financially supported by Kansai Research Foundation for technology promotion.

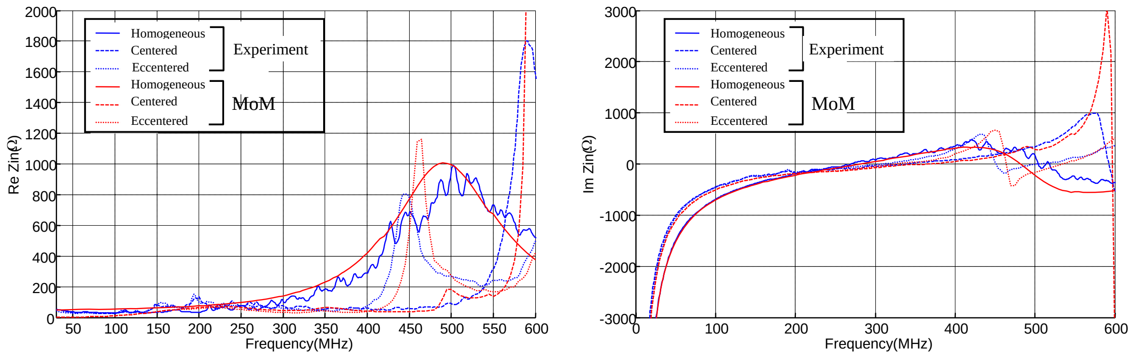

(a) (b)

Figure 3: Input impedance Z_{in} of the dipole antenna. (a) Resistance. (b) Reactance. The total length l and radius a of the dipole antenna are 0.5 m and 5 mm, respectively. $\rho' = 0\,\mathrm{mm}$ in "Centered" and $\rho' = 9\,\mathrm{mm}$ in "Eccentered". The parameters for both "Centered" and "Eccentered": $a_1 = 2\,\mathrm{cm}$, $a_2 = 3.2\,\mathrm{cm}$, $\varepsilon_{r1} = \varepsilon_{r3} = 1$, $\varepsilon_{r2} = 80$, $\sigma_1 = \sigma_2 = \sigma_3 = 0\,\mathrm{S/m}$. In "Homogeneous", there are no cylindrical interfaces and the surrounding medium is air only. In the experimental data, the measured input impedance of the monopole antenna in Fig. 4 was multiplied by 2 in order to compare the experimental input impedance of the dipole antenna calculated with the MoM.

References

[1] S. Ebihara, "Directional borehole radar with dipole antenna array using optical modulators ," *IEEE Trans. on Geoscience and Remote Sensing*, Vol. 42, No. 1, pp. 45 -58, January 2004.

[2] S. Ebihara, and T. Yamamoto "Resonance Analysis of Circular Dipole Array Antenna in Cylindrically Layered Media for Directional Borehole Radar," *IEEE Trans. Geosci. Remote Sens.*, Vol. 44, No. 1, pp. 22-31, January 2006.

[3] S. Ebihara and Y. Hashimoto, "MoM Analysis of Dipole Antennas in Crosshole Borehole Radar, and Field Experiments," *IEEE Transactions on Geoscience and Remote Sensing* (to be published).

[4] J. R. Lovell and W. C. Chew, "Effect of tool eccentricity on some electrical well-logging tools," *IEEE Transactions on Geoscience and Remote Sensing*, vol. 28, no. 1, pp. 127-136, Jan. 1990.

[5] Y. Hue and F. L. Teixeira, "Analysis of tilted-coil eccentric borehole antennas in cylindrical multilayered formations for well-logging applications," *IEEE Transactions on Antennas and Propagation*, vol. 54, no. 4, pp. 1058-1064, April 2006.

[6] W. C. Chew, *Waves and Field in Inhomogeneous Media*, New York, IEEE Press, 1995.